# DESIGN AND ANALYSIS OF A 3.5 GHZ INSET-FED RECTANGULAR MICROSTRIP PATCH ANTENNA WITH I-SLOT AND AIR GAP FOR SUB-6 GHZ 5G APPLICATIONS

**Isah, M.M.[1*] and Chinedu, P.U.[2]**

[1]Department of Computer Engineering, Edo State University Iyamho, Edo State, Nigeria

[2]Department of Information Systems and Technology, Southern Delta University, Ozoro, Delta State, Nigeria

*Corresponding email: isah.m.m@gmail.com

**ABSTRACT**

*This paper presents the design and analysis of an inset-fed rectangular microstrip patch antenna operating at 3.5 GHz. The proposed antenna incorporates two key modifications to enhance performance beyond that of a conventional patch: an I-shaped slot cut into the radiating patch and a suspended structure that introduces a 2 mm air gap between the patch and the ground plane. The antenna is fed via an inset configuration to achieve direct matching to a 50 Ω system without additional matching components. Design parameters were calculated using the transmission line model equations, and the antenna's performance was evaluated in terms of return loss, bandwidth, gain, and directivity. The introduction of the air gap lowers the effective dielectric constant and reduces dielectric and conductor losses, while the I-slot perturbs the surface current distribution, creating additional resonant modes. The simulation was performed using CST Studio Suite 2025, a commercially available Computer Simulation Technology product for patch antenna simulation. The proposed antenna achieves a maximum gain of 5.278 dBi and a maximum directivity of 6.584 dBi, with a bandwidth of 63 MHz spanning 3.469-3.533 GHz. These results demonstrate that the proposed design is suitable for 3.5 GHz in sub-6 GHz 5G wireless communication applications.*

**Keywords**: Microstrip patch antenna, inset feed, I-shaped slot, suspended structure, air gap, 3.5 GHz

## 1 INTRODUCTION

The concept of the microstrip patch antenna originated in the 1950s, but it did not attract serious attention until the 1970s. Since then, thousands of papers have been written on microstrip patch antennas [1]. Microstrip antennas have the advantages of low cost, compact size, etc. [1, 2, 3, 4, 5], making them suitable for various applications in mobile communication [6]. However, the microstrip antenna has some disadvantages, including low bandwidth and low gain [3, 4]. Researchers have proposed several techniques for enhancing the properties of ordinary microstrip antennas in their native form; these techniques include stacking [7], different feeding techniques [4], [8], Frequency Selective Surfaces (FSS) [9, 10], Electromagnetic Band Gap (EBG) [11, 12], Photonic Band Gap (PBG) [13, 14], Defective Ground Surface (DGS) [15, 16], Metamaterial [17, 18], etc. The various methods mentioned were intended to improve the major problems of patch antennas. Significant progress has been achieved in this direction, and patch antennas have gained popularity in many IoT-based designs of the 21st century [19, 20, 21]. To improve the performance of microstrip antennas for various applications, [21] investigated the miniaturisation of a microstrip patch antenna. The authors targeted the WiMAX frequency band by introducing slot configurations in both the patch geometry and the

ground plane. This modification successfully shifted the resonant frequency downward from 5.2 GHz to the 3.5 GHz WiMAX band without increasing the antenna's physical dimensions. The dual-surface slotting technique altered the surface current distribution, enabling a 54% reduction in physical size while maintaining stable impedance matching, satisfactory return loss, and adequate radiation characteristics required for WiMAX applications. Researchers in [22] investigated the design of a compact dual-band microstrip patch antenna targeting simultaneous sub-6 GHz 5G and WiMAX communications. It utilises a cost-effective FR-4 substrate to implement a localised, geometrically slotted configuration on the patch structure. This configuration establishes alternate, independent electrical current paths. This architectural modification enabled the antenna to overcome single-resonance limitations, successfully securing distinct, stable dual-operating bands at the 3.5 GHz WiMAX and 5.2 GHz sub-6 GHz 5G frequencies. Also, [23] designed a 3.5 GHz microstrip patch antenna for S-band wireless communication using a Rogers RT/duroid 5880 substrate with a dielectric permittivity of 2.2. Evaluations in CST Studio Suite revealed an exceptional return loss of −50.423 dB, a near-ideal VSWR of 1.0061, a directivity of 7.43 dBi, and a bandwidth of 122.1 MHz. [24] present a compact triple-slotted rectangular microstrip patch antenna with a metamaterial ground plane for Sub-6 GHz/5G communication. The triple-slot configuration and metamaterial ground are used to miniaturise the antenna and enhance its performance. The design is characterised for Sub-6 GHz 5G applications, demonstrating compact size and suitable radiation characteristics for next-generation wireless communication systems. In [25], a multiple-microstrip dipole antenna that achieves a good gain of 8.9 dBi and a bandwidth of 1.07 GHz was proposed. [26] Present a low-profile aperture-coupled antenna was proposed. The antenna exhibits an enhanced bandwidth of 15.2% while maintaining a low profile and a gain of 6.8 dBi. In [27], a low-profile, high-gain filtering antenna based on a nonuniform metasurface for fifth-generation (5G) systems was proposed. The antenna uses a Rogers RO4003C substrate ($\varepsilon r = 3.38$, $\tan \delta = 0.0027$) and a Taconic TLX-9 substrate ($\varepsilon r = 2.5$, $\tan \delta = 0.0019$), respectively. The proposed antenna has a bandwidth of 15.91% and a maximum gain of 10.43 dBi. A circular patch antenna design with a high gain using a novel artificial planar dual-layer metamaterial superstrate was proposed [28]. The design has a 30% bandwidth and a maximum gain of 7.5dBi while maintaining a total volume of $1.01\lambda g \times 1.01\lambda g \times 0.025\lambda g$. [29] Presented a 2.4 GHz metamaterial microstrip patch antenna. Their design enhances the performance of conventional patch antennas. The antenna used an FR4 Epoxy substrate, achieving a return loss of -46.58 dB, a VSWR of 1.009, a bandwidth of 574 MHz, a directivity of 3.379 dBi, and a gain of 3.23 dBi at a resonant frequency of 2.4 GHz. In fabrication and testing, the antenna achieved a VSWR of 1.3, return loss of -26 dB, and bandwidth of 200 MHz, making it suitable for 2.4 GHz WiFi applications. This paper presents an inset-fed rectangular microstrip patch antenna operating at 3.5 GHz. Two modifications enhance performance beyond a conventional patch: an I-shaped slot in the radiating patch and a suspended structure with a 2 mm air gap above the ground plane. The inset feed provides direct 50 Ω matching without extra components. Design parameters were derived using transmission line model equations, and performance was evaluated in terms of return loss, bandwidth, gain, and directivity. The air gap reduces dielectric and conductor losses, while the I-slot perturbs surface currents to create additional resonant modes.

## 2 Design of the Proposed Antenna

The proposed antenna is a rectangular microstrip patch antenna. It is fed via an inset configuration to match a 50 Ω input impedance. This feeding method was selected because it enables straightforward impedance matching without additional matching components, keeping the design simple and efficient [30]. To improve performance beyond that of a conventional patch, two key modifications are incorporated: an I-shaped slot is cut into the patch, and the antenna is suspended by 2 mm above the bottom plate to create an air gap, rather than being printed directly on a solid dielectric [31]. The 2 mm air gap between the antenna top design and the substrate and ground plane of the bottom design is a deliberate design choice intended to overcome the typical limitations of microstrip antennas. Conventional patch antennas fabricated on solid substrates exhibit an inherently narrow bandwidth. By introducing an air gap, which has a dielectric constant of unity, a suspended configuration is created that substantially increases the impedance bandwidth [31]. Furthermore, because air exhibits virtually no dielectric loss, suspending the antenna reduces the medium's effective dielectric constant. This diverts electromagnetic energy away from the lossy substrate and ground plane, thereby lowering

conductor and dielectric losses and improving overall efficiency. The copper ground plane serves as the antenna's reflective backplane. It reflects electromagnetic waves that would otherwise radiate downward, directing the energy upward to form the antenna's radiation pattern. In a microstrip design, the ground plane also interacts with the feed line and patch to establish the characteristic impedance, in this case, the 50 Ω match. The substrate, or bottom plate, is the dielectric layer situated beneath the patch and above the air gap in this suspended configuration. It provides a rigid physical base for the antenna structure, supporting the feed network and the ground plane. Electrically, although the air gap reduces the effective dielectric constant, the substrate still influences the field distribution; in a suspended design, the substrate thickness and its properties help determine the resonant frequency and can be tuned to optimise the radiation characteristics [31]. The air gap was optimised between 0 mm and 2 mm. During optimisation, the antenna performed best at 2 mm, improving the proposed antenna's gain from 4.698 dB to 5.278 dB. The antenna is designed to resonate at 3.5 GHz, with its physical properties calculated using the transmission line model equations [3]. The design equations governing the rectangular microstrip patch antenna are presented below.

$$W = \frac{c}{2 f_r} \sqrt{\frac{2}{\epsilon_r + 1}} \tag{1}$$

W, c, fr, and εr are the patch width, speed of light, resonant frequency, and dielectric constant of the substrate, respectively. Equations (2) and (3) produce the effective dielectric constant $\varepsilon_{reff}$ due to the fringing effect and the effective length of the patch L.

$$\epsilon_{reff} = \frac{\epsilon_r + 1}{2} + \frac{\epsilon_r - 1}{2\sqrt{1 + \frac{12h}{W}}} \tag{2}$$

$$L = L_{eff} - 2\Delta L = \frac{c}{2 f_r \sqrt{\epsilon_{reff}}} - 2\Delta L \tag{3}$$

Where $\Delta L$ is given by:

$$\Delta L = \frac{h(0.412)\left(\left(\epsilon_{reff} + 0.3\right)\left(\frac{W}{h} + 0.264\right)\right)}{\left(\epsilon_{reff} - 0.258\right)\left(\frac{W}{h} + 0.8\right)} \tag{4}$$

Where h is the substrate height or thickness; for this design, the substrate height is 0.762 mm, the dielectric constant is 3.66, and the radiating frequency is 3.5 GHz [3]. Figure 1 (a) shows the front of the patch. Figure 1 (b) shows the back end of the antenna. The figure shows that the antenna patch has an I-slot in the middle to enhance the design's performance.

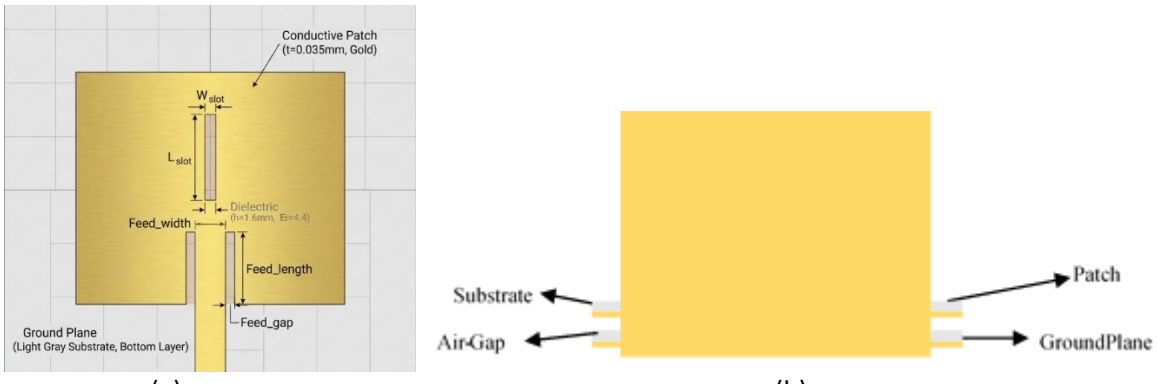


(a) (b)

Figure 1. (a) Top view (b) Back view of the proposed patch antenna (c) Side view of the proposed antenna

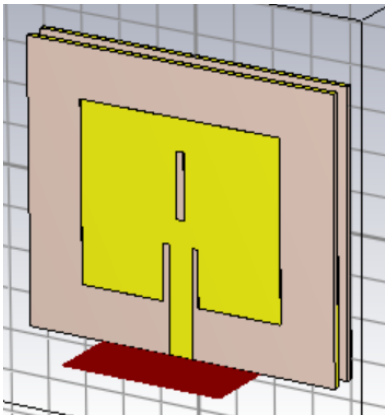

Figure 2. Optimised antenna design from CST Studio

Table 1 shows the optimised antenna parameters. The design equations 1-4 are used to calculate the antenna parameters. The antenna's width, length, patch width, and height are calculated using the equations. During the antenna simulation in the CST Studio Suite, it was observed that some tuning was necessary to obtain the optimal parameter values, as shown in Table 1.

Table 1. Antenna Parameters

| Parameter | Wp | Lp | h | Gfi |
|---|---|---|---|---|
| Value (mm) | 26.05 | 22.25 | 0.762 | 0.777 |
| Parameter | Wg | Lg | Fi | Wf |
| Value (mm) | 40 | 35 | 7 | 3.0 |
| Parameter | Sl | Sw | hc | aig |
| Value (mm) | 12 | 2 | 0.035 | 2 |
| Parameter | $\varepsilon$ | | | |
| Value (mm) | 3.66 | | | |

## 3 RESULTS AND DISCUSSIONS

### 3.1 Reflection Coefficient (S11) Plot

Figure 3 illustrates the simulated reflection coefficient (S11) for the three design iterations. All three antennas exhibit a strong resonance centred exactly at the target 3.50 GHz, achieving excellent impedance matching with S11 values below -26 dB. The integration of the central I-slot and the suspended air gap does not degrade the fundamental impedance match. Furthermore, the final air-gap design exhibits a smoother, slightly wider -10 dB bandwidth compared to the narrowband baseline, demonstrating the effectiveness of the combined slot-and-air-gap architecture.

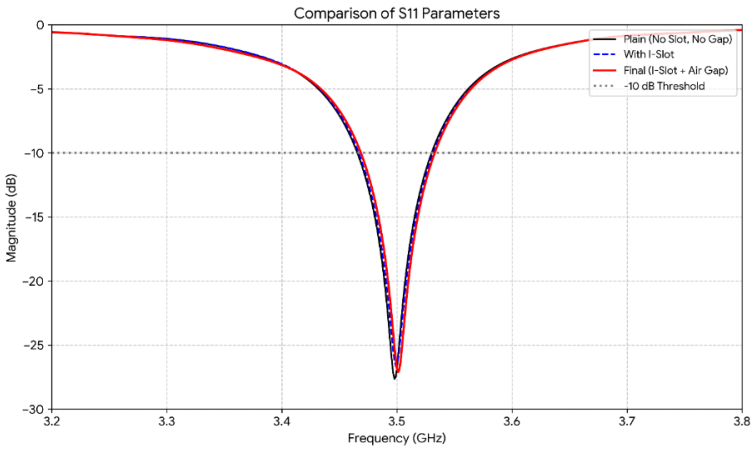


Figure 3. Combined S11 plots of the three designs

### 3.2 Voltage Standing Wave Ratio (VSWR) of the Three Designs

Figure 4 presents the simulated Voltage Standing Wave Ratio (VSWR) for the baseline, slotted, and final air-gap antennas. All three designs exhibit a sharp resonance centred precisely at the target 3.50 GHz, dipping well below the standard industrial threshold of VSWR < 2.0. The final proposed design achieves an exceptional minimum VSWR of 1.09, which corresponds to an S11 of -27.1 dB, confirming a nearly perfect 50-ohm impedance match. The VSWR curve of the final design perfectly overlaps the baseline at the centre frequency, visually demonstrating that the structural modifications do not degrade the fundamental impedance characteristics. Furthermore, the final air-gap design exhibits a slightly wider and smoother curve at the VSWR = 2.0 crossing, indicating a minor enhancement in operational bandwidth compared to the narrowband baseline.

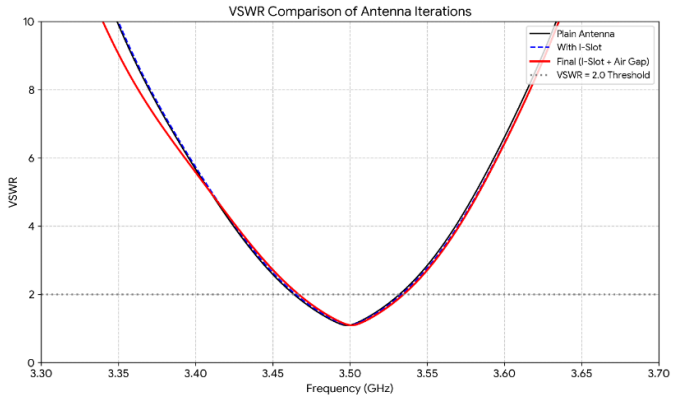


Figure 4. VSWR of the three designs

### 3.3 Efficiency Analysis of the Design

The radiation and total efficiencies of the three design iterations, plain antenna, I-Slotted antenna, and the Final Design (Slotted + Air Gap), were analysed across the 3.42 GHz - 3.58 GHz band, as shown in Figure 5.

#### *3.3.1 Radiation Efficiency*

The radiation efficiency (η rad) measures the antenna's ability to radiate the power it accepts. This parameter is independent of impedance mismatch. As observed in Figure 4(a), all three designs maintain a highly stable radiation efficiency of approximately 74% to 75% (-1.26 dB to -1.30 dB) at the target frequency of 3.5 GHz. The transition of the antenna from the plain patch design to the final air-gap design results in a mathematically negligible drop in radiation efficiency (from -1.265 dB to -1.297 dB, a difference of 0.03 dB or <1%). This shows that neither the etching of the I-slot nor the introduction of the suspended air-gap design introduces significant dielectric or ohmic losses. The high and consistent radiation efficiency across all iterations validates the choice of the low-loss RO4350B substrate.

#### *3.3.2 Total Efficiency*

The total efficiency (η total) accounts for both the radiation efficiency and the impedance mismatch (reflection loss). As depicted in Figure 4(b), all three designs exhibit a distinct peak centred exactly at 3.50 GHz, reaching approximately 73.8% to 74.6% (-1.27 dB to -1.31 dB). At 3.5 GHz, the total efficiency closely matches the radiation efficiency for all iterations. This narrow gap indicates excellent impedance matching (S11 < -20 dB) at the centre frequency, demonstrating that the inset feed dimensions successfully maintain a 50-ohm match regardless of the design. Moving away from 3.5 GHz, the total efficiency drops sharply (down to ~-3.7 dB at 3.58 GHz) due to the inherently narrowband nature of the fundamental TM10 mode.

#### *3.3.3 Justification of the I-Slot and Air Gap*

While the efficiency plots show a slight numerical decrease for the final design, the design justification for the I-slot and the air gap lies in spectral purity and radiation pattern optimisation, rather than raw efficiency. The slotted design (with and without the air gap) exhibits nearly identical efficiency

curves to the plain baseline (e.g., -1.264 dB vs -1.265 dB at 3.5 GHz). This proves that the I-slot does not degrade the fundamental mode. Instead, its structural purpose is to act as a localised impedance barrier. This diverts the longitudinal surface currents and prevents the excitation of higher-order modes without degrading the fundamental radiation efficiency. The final addition of the 2 mm air gap results in a negligible 0.04 dB reduction in efficiency. This minor trade-off is entirely justified by the drastic improvements in the far-field radiation pattern. The suspended air gap lowers the effective dielectric constant, thereby reducing surface-wave excitation and suppressing parasitic substrate coupling. As a result, the final design achieves a highly focused, directional beam with an exceptional Side Lobe Level (SLL) of -20.8 dB (compared to -11.8 dB in the baseline) and a realised gain of 5.28 dBi. The efficiency data demonstrate that the proposed antenna operates near the theoretical limit for the Rogers RO4350B substrate (Approx. 75%). The minor 0.04 dB difference is a highly favourable engineering trade-off: the final design sacrifices a negligible fraction of efficiency to achieve a significantly cleaner, highly directional radiation pattern, making it vastly superior for 5G communication systems.

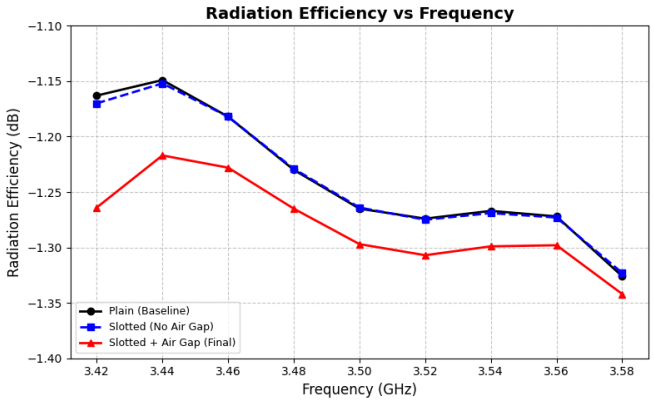


Figure 5(a). Antenna radiation efficiency

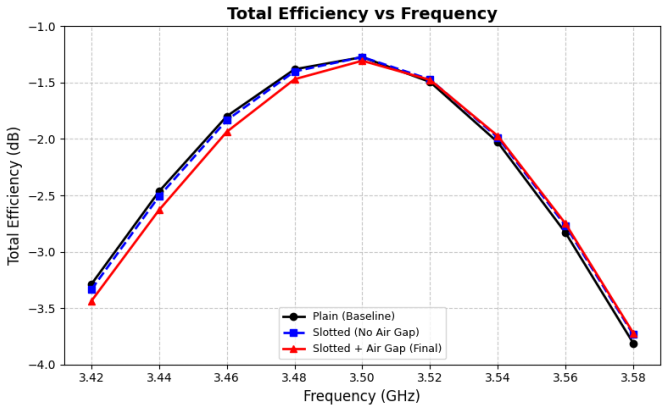


Figure 5(b). Antenna total efficiency

### 3.4 Surface Current Distribution and Radiation Mechanism

The surface current distributions for the three designs were simulated at 3.5GHz, the fundamental operating frequency, to assess impedance matching and radiation performance as shown in Figure 6. The baseline version of the design is shown in Figure 6(a); the currents flow uniformly from the inset feedline to the patch's upper edge. A pronounced current buildup is evident along the left and right vertical boundaries, the main radiating edges, indicating that the fundamental TM10 mode is excited. A major problem here is the high dielectric loss, which dampens the efficient radiation of the fringing fields. The introduction of the I-slot in the centre alters the current path considerably, as shown in Figure 6(b). The vertical currents emanating from the feedline must be routed around the slot, thereby establishing a region of high localised impedance. The modification does lead to some complex interaction in the vicinity of the slot, but the bulk of the current along the left and right radiating edges is undisturbed. As a result, the slot serves as an effective structural filter, preserving the 3.5GHz resonance. A much more refined current distribution is observed in the final design, where both the I-

slot and a 2 mm suspended air gap are in place, as shown in Figure 6(c). The air gap lowers the medium's equivalent dielectric constant, keeping dielectric losses and surface-wave excitation to a minimum. The electromagnetic fields are not retained in the lossy substrate as before; instead, they couple well to the ground plane. As shown in Figure 6(c), the currents are tightly focused at the radiating edges, with minimal parasitic dissipation. This optimisation of the current flow is what gives the finished prototype its improved radiation efficiency and a highly directional pattern with low Side Lobe Level (SLL = -20.8 dB).

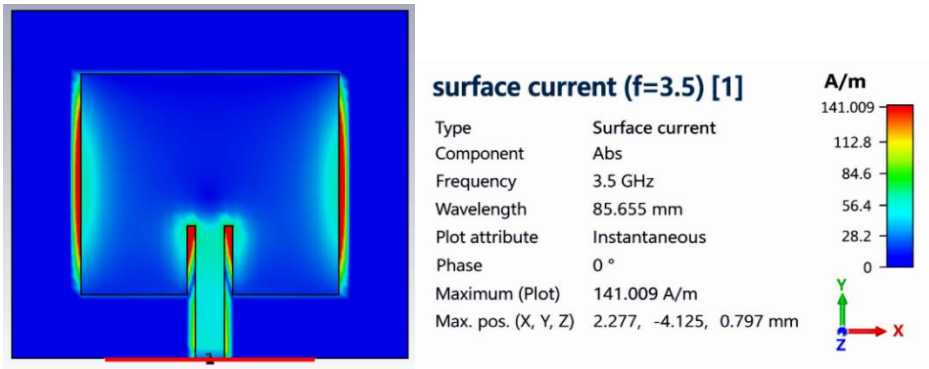


Figure 6(a). Surface current distribution of the Baseline design at 3.5 GHz, showing the fundamental mode

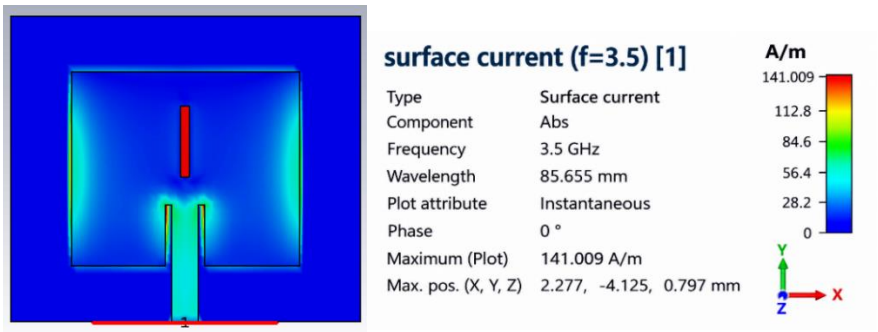


Figure 6(b). Surface current distribution of the I-Slotted Design at 3.5 GHz, showing the fundamental mode

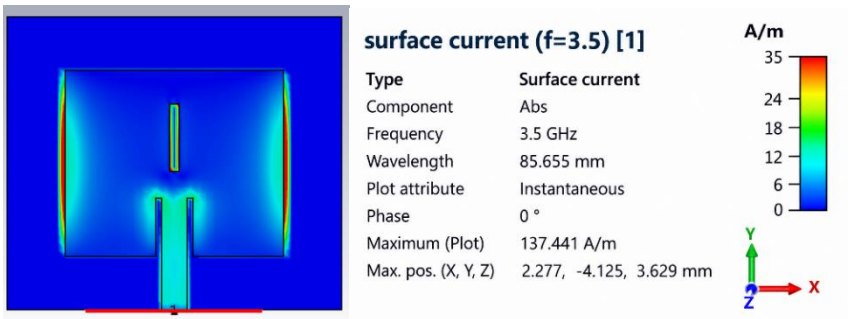


Figure 6(c). Surface current distribution of the proposed I-Slotted antenna with air-Gap at 3.5 GHz, showing the fundamental mode

### 3.5 Far-Field Radiation Pattern Analysis

The simulated 2D farfield radiation patterns at 3.50 GHz were analysed for both the Phi = 90° and Phi = 0° planes, as shown in Figure 7. All three design iterations exhibit a prominent broadside main lobe centred precisely at Theta = 0°, shown in Figure 6(c), confirming the dominant excitation of the fundamental TM10 mode. However, significant differences are observed in the side-lobe and back-lobe regions. In both principal planes, the baseline Plain Antenna (black curve) and the Slotted Antenna (blue curve) exhibit substantial backward and lateral radiation (between 90° and 180°). In contrast, the final proposed design incorporating the suspended air gap (red curve) demonstrates a highly directional and symmetrical pattern. The air gap effectively suppresses the excitation of surface waves within the

substrate, resulting in a drastically reduced back-lobe level and a tighter beamwidth. The sharp nulls observed at Theta = 90° (in both planes) and the pronounced notch at Theta = 180° (in the Phi = 0° plane) confirm that the final design minimises parasitic backward radiation. This highly focused, forward-directed radiation makes the proposed antenna exceptionally well-suited for interference-sensitive 5G applications. The performance comparison of the proposed design and some related literatures are shown in Table 1.

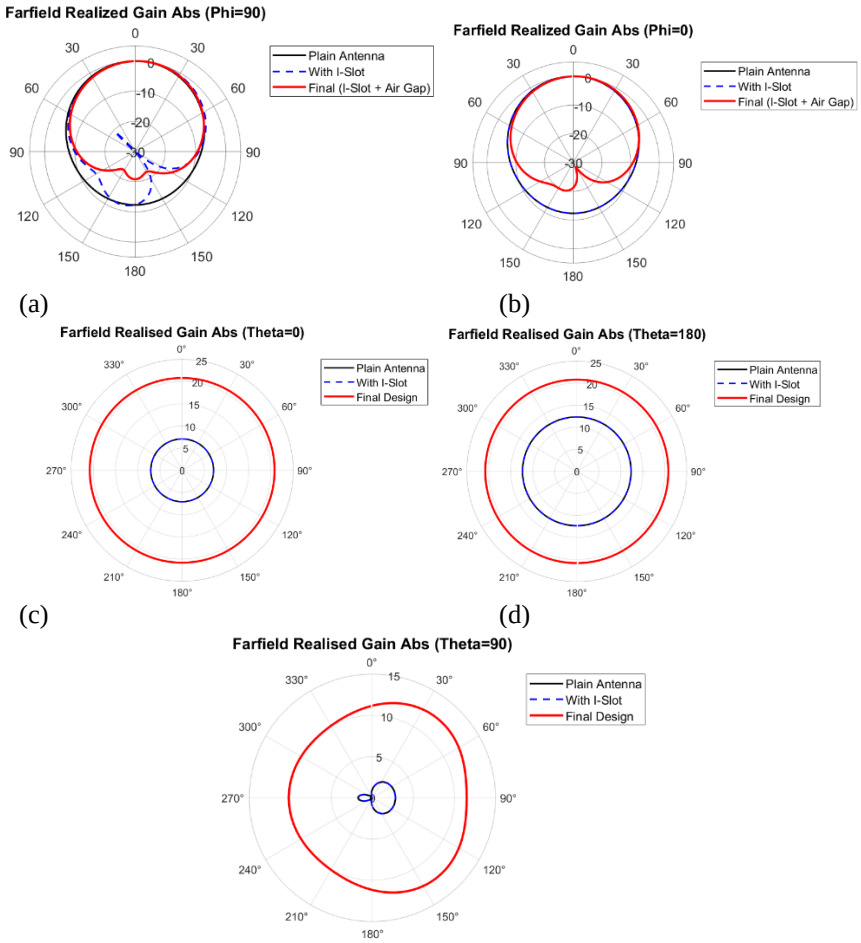


Figure 7. Antenna radiation properties at 3.5GHz.

### 3.6 Performance Comparison Table

Table 2. Performance comparison of the proposed antenna with some cited work.

| Reference / Design | Substrate Material | Freq (GHz) | Gain (dBi) | Rad. Efficiency | SLL |
|---|---|---|---|---|---|
| Ref [23] | Duroid 5880 | 3.5 | 3.0 to 4.0 | < 60% | N/R |
| Ref [15] | FR-4 | 5.0 | > 6 | 65% | -12 |
| Ref [21] | FR-4 | 3.5 | 3.7 | < 50% | N/R |
| Ref [22] | FR-4 | 3.5, 5.1 | 2.0 to 4.0 | N/R | N/R |
| Proposed design | RO4350B + Air Gap | 3.5 | 5.28 | 75% | -20.8 dB |

## 4 CONCLUSIONS

This paper presented a high-performance patch antenna for 3.5 GHz 5G applications, addressing the limitations of conventional designs. The proposed architecture uses a low-loss Rogers RO4350B substrate, improving radiation efficiency to 75%. Also, a central I-slot was etched into the patch, successfully suppressing higher-order modes without disturbing the fundamental resonance. Furthermore, a 2 mm suspended air gap was introduced to enhance spatial purity. While the air gap resulted in a negligible efficiency drop of 0.03 dB, it drastically improved the far-field pattern. The final

optimised antenna achieved an excellent impedance match (S11 = -27.1 dB), a realised gain of 5.28 dBi, and a side-lobe level (SLL) of -20.8 dB, significantly outperforming the baseline (-11.8 dB). The proposed design offers a highly directional, interference-resistant solution for modern 5G systems.

## REFERENCES


1. Lee, K.F. (2016). A personal overview of the development of microstrip patch antennas. *IEEE International Symposium on Antennas and Propagation (APSURSI). IEEE Conference Publications*, pp. 689-690.
2. Ngobese, B. and Kumar, P. (2018). A high gain microstrip patch array for 5 GHz WLAN applications. *Adv. Electromagn*., vol. 7, no. 3, pp. 93-98.
3. Balanis, C.A. (2024). Balanis' advanced engineering electromagnetics. *John Wiley & Sons, Hoboken, NJ.*
4. Ahmed, M.F. and Kabir, M.H. (2026). Microstrip Patch Antennas for Wireless Communication: A Comprehensive Review of Bandwidth and Gain Enhancement Techniques and Feeding Methods. *Facta Univ. Ser. Electron. Energ*., vol. 39, no. 3, pp. 601-628.
5. Momoh, M.O., Ibe, C.C., Mohammed, A., Abbe, G.E., Ter, K.P., Obari, J.A. and Bulama, H.I. (2025). A Low-cost Antenna Tracking System Integrated with GPS for UAVs. *Computer Engineering & Applications Journal*, vol. 14, no. 3, pp. 239-251.
6. Ayo-Bello, O., Aibinu, A.M., Ubadike, O., Onumanyi, A.J. and Momoh, M.O. (2022). A QoS Estimation Algorithm from Caller Ringtone Analysis in GSM Network. *Int. J. Softw. Eng. Comput. Syst*., vol. 8, no. 1, pp. 53-68.
7. Tian, A., Liu, C., Hernández-Escobar, A., Kojima, T., Sakai, H., Kunihiro, K., Tomura, T. and Okada, K. (2026). A 110-170 GHz Stacked-PCB-Based Pyramidal Horn Antenna with Flexible Stacking. *IEEE Trans. Terahertz Sci. Technol*., pp. 555-563.
8. Akinola, S., Hashimu, I. and Singh, G. (2019). Gain and bandwidth enhancement techniques of microstrip antenna: a technical review. *International Conference on Computational Intelligence and Knowledge Economy (ICCIKE), IEEE*, pp. 175-180.
9. Mohamed, H.A., Edries, M., Abdelghany, M.A. and Ibrahim, A.A. (2022). Millimeter-wave antenna with gain improvement utilizing reflection FSS for 5G networks. *IEEE Access*, vol. 10, pp. 73601-73609.
10. Shi, C., Zou, J., Gao, J. and Liu, C. (2022). Gain enhancement of a dual-band antenna with the FSS. *Electronics*, vol. 11, no. 18, p. 1-15.
11. Hyunjae, L. and Sungho, J. (2026). Performance Enhancement of Planar Antennas Using Electromagnetic Bandgap Structures for Interference Suppression. *J. Adv. Antenna RF Eng*., vol. 2, no. 2, pp. 22-33.
12. Zuo, P., Yang, H., Chen, M., Hu, Z., Li, T., Liu, G., Yang, L. and Li, E.P. (2026). Suppression for UWB Simultaneous Switching Noise by Electromagnetic Bandgap with Helix Defected Ground Structure. *IEEE Trans. Electromagn. Compat*.
13. Qian, Y., Coccioli, R., Sievenpiper, D., Radisic, V., Yablonovitch, E. and Itoh, T. (1999). A microstrip patch antenna using novel photonic band-gap structures. *Microw. J.*, vol. 42, no. 1, pp. 66-72.
14. Rahaman, R., Ahammed, B., Shuhrawardy, M. and Alim, M.A. (2026). Photonic band Gap-Based different slot patch antenna with Machine learning Verification for Wi-Fi 5/6. *Eng. Sci. Technol. Int.* J., vol. 80, pp. 102456.
15. Olawoye, T.O. and Kumar, P. (2020). A high-gain microstrip patch antenna with slotted ground plane for sub-6 GHz 5G communications. *International Conference on Artificial Intelligence, Big Data, Computing and Data Communication Systems (icABCD), IEEE*, pp. 1-6.

16. Abubakre, O.R., Ubadike, O., Aibinu, A.M., Folorunso, T.A. and Momoh, M.O. (2021). Artificial neural network embedded optimal mobile communication system. *Covenant J. Informatics Commun. Technol*., vol. 9, no. 2, pp. 1-10.

17. Kumar, P., Ali, T. and Pai, M.M. (2021). Electromagnetic metamaterials: A new paradigm of antenna design. *IEEE Access*, vol. 9, pp. 18722-18751.

18. Ajewole, B., Kumar, P. and Afullo, T. (2022). I-shaped metamaterial using SRR for multi-band wireless communication. *Crystals*, vol. 12, no. 4, pp. 559.

19. Islam, M.S., Islam, M.T., Ullah, M.A., Beng, G.K., Amin, N. and Misran, N. (2019). A modified meander line microstrip patch antenna with enhanced bandwidth for 2.4 GHz ISM-band Internet of Things (IoT) applications. *IEEE Access*, vol. 7, pp. 127850-127861.

20. Zambak, M.F., Al-Bawri, S.S., Jusoh, M., Rambe, A.H., Vettikalladi, H., Albishi, A.M. and Himdi, M. (2023). A compact 2.4 GHz L-shaped microstrip patch antenna for ISM-band Internet of Things (IoT) applications. *Electronics*, vol. 12, no. 9, pp. 21-49.

21. Chakraborty, S., Gangapadhyaya, M., Sinha, B. and Chakraborty, M. (2018). Miniaturization of rectangular microstrip antenna at WiMAX band with slot in patch and ground surface. *2nd International Conference on Electronics, Materials Engineering & Nano-Technology (IEMENTech), IEEE*, 2018, pp. 1-5.

22. Suganyadevi, S., Priyadharsini, S., Raaghul Ganesh, S., Ramakrishnan, R., Sowmiya, R. and Srinithi, P. (2024). Design of a compact dual band antenna for 5G and WiMAX applications. *Third International Conference on Distributed Computing and Electrical Circuits and Electronics (ICDCECE), IEEE*, 2024, pp. 1-6.

23. Rana, M.S., Fahim, T.A., Ghosh, B. and Rahman, M.M. (2023). Microstrip patch antenna design and simulation for S-band wireless applications operating at 3.5 GHz. *Bull. Electr. Eng. Inform*., vol. 12, no. 6, pp. 3428-3437.

24. Vinoth, M. and Vallikannu, R. (2020). A compact triple slotted Rectangular Microstrip Patch Antenna with Metamaterial ground for Sub-6 GHz/5G communication. *Fifth International Conference on Research in Computational Intelligence and Communication Networks (ICRCICN), IEEE*, 2020, pp. 34-38.

25. Zhou, Z., Wei, Z., Tang, Z. and Yin, Y. (2019). Design and analysis of a wideband multiple-microstrip dipole antenna with high isolation. *IEEE Antennas Wirel. Propag. Lett*., vol. 18, no. 4, pp. 722-726.

26. Liu, N.W., Zhu, L., Choi, W.W. and Zhang, X. (2017). A low-profile aperture-coupled microstrip antenna with enhanced bandwidth under dual resonance. *IEEE Trans. Antennas Propag*., vol. 65, no. 3, pp. 1055-1062.

27. Park, J., Jeong, M., Hussain, N., Rhee, S., Park, S. and Kim, N. (2019). A low-profile high-gain filtering antenna for fifth generation systems based on nonuniform metasurface. *Microw. Opt. Technol. Lett*., vol. 61, no. 11, pp. 2513-2519.

28. El Yassini, A., Aguni, L., Ibnyaich, S., Chabaa, S. and Zeroual, A. (2019). Design of circular patch antenna with a high gain by using a novel artificial planar dual-layer metamaterial superstrate. *Int. J. RF Microw. Comput.-Aided Eng*., vol. 29, no. 11, pp. 120-130.

29. Geetharamani, G. and Aathmanesan, T. (2020). Design of metamaterial antenna for 2.4 GHz WiFi applications. *Wirel. Pers. Commun*., vol. 113, no. 4, pp. 2289-2300.

30. Bansal, A. and *Gupta, R. (2020). A review on microstrip patch antenna and feeding techniques. Int*. J. Inf. Technol., vol. 12, no. 1, pp. 149-154.

31. Sandi, E., Maruddani, B. and Betakore, S. (2021). Gain enhancement by using combination slot techniques for millimeter-wave 5G antenna. *IOP Conference Series: Materials Science and Engineering, IOP Publishing*, pp. 042091.